Reaction Chemistry & Engineering

Effect of Metal Chlorides on Glucose Mutarotation and Possible Implications on Humin Formation

Journal:	*Reaction Chemistry & Engineering*
Manuscript ID	RE-COM-10-2018-000233.R1
Article Type:	Communication
Date Submitted by the Author:	28-Nov-2018

Complete List of Authors:	Ramesh, Pranav; Rutgers The State University of New Jersey, Chemical and Biochemical Engineering Kritikos, Athanasios; Rutgers The State University of New Jersey, Chemical and Biochemical Engineering Tsilomelekis, George; Rutgers The State University of New Jersey, Chemical and Biochemical Engineering

Journal Name

COMMUNICATION

Effect of Metal Chlorides on Glucose Mutarotation and Possible Implications on Humin Formation

Pranav Ramesh[a], Athanasios Kritikos[a] and George Tsilomelekis[a]*

Received 00th January 20xx,
Accepted 00th January 20xx

DOI: 10.1039/x0xx00000x

www.rsc.org/

An in-situ Raman spectroscopic kinetic study of the glucose mutarotation reaction is presented herein. The effect of metal chlorides on the ease of ring opening process is discussed. It is shown that $SnCl_4$ facilitates the mutarotation process towards the β-anomer extremely fast, while $CrCl_3$ appears to promote the formation of the α-anomer of glucose. Infrared spectra of humins prepared in different Lewis acids underscore the posibility of multiple reaction pathways.

Introduction

Converting biomass, a renewable source of carbon, to value-added products is a promising and sustainable approach for biofuel/biochemical production with immense benefits to several industrial sectors. Carbohydrates, aldoses and/or ketoses, derived from the cellulosic/hemicellulosic constituents of non-edible biomass sources comprise excellent candidates for chemical production but the high oxygen content in their structure require further downstream process[1, 2]. The pivotal impact of the selective conversion of these monosaccharides to their dehydration counterparts as intermediates has been underscored in recent years[3, 4]. A characteristic example encompasses the conversion of cellulose derived glucose to 5-Hydroxymethylfurfural (5-HMF) which is considered as one of the key biomass-derived intermediates.

Glucose isomerization to fructose is an important intermediate reaction in the production of 5-Hydroxymethylfurfural from cellulosic biomass sources and is well established that is Lewis acid catalyzed. The presence of Lewis acids is believed to facilitate glucose ring-opening in aqueous solution followed by a kinetic relevant intramolecular hydride shift from C_2 to the C_1 position of glucose[5]. The ease of the first step, i.e. ring opening, in the presence of metal chlorides in ionic liquids have been reported by means of DFT calculations[6]. It has also been suggested that the possible changes in the anomeric equilibrium especially via the stabilization of the α-anomer of glucose, might be responsible for improved selectivity towards fructose[7, 8]. This also agrees with the concept of anomeric specificity of enzymes; for instance, immobilized D-glucose isomerase has shown ~40% and ~110% higher conversion rates starting with α–D-glucose as compared to equilibrated glucose and β–D-glucose solutions respectively[9]. Production of 5-HMF in ~60% yields has been reported by coupling homogeneous Lewis with Bronsted acids in a tandem glucose isomerization and fructose dehydration scheme (scheme S1)[10].

Herein, we report an in-situ Raman kinetic study on the ease of glucose mutarotation in the presence of $AlCL_3$, $CrCl_3$ and $SnCl_4$ homogeneous Lewis acid catalysts. The rationale behind choosing these metal salts lies at the fact that although all three salts have proven to facilitate glucose isomerization under various reaction conditions product distribution varies significantly, with $AlCl_3$ and $CrCl_3$ to be more selective. $SnCl_4$ has reported to facilitate glucose isomerization reaction at the 130-150°C temperature range; however, the process suffers from significant formation of side reactions (humins) thus sacrificing product selectivity. We believe that metal chlorides as Lewis acids, can potentially affect product selectivity in biomass reactions by altering a) the kinetics of ring opening and b) the equilibrium level of the mutarotation process as well as by c) introducing additional pathways towards degradation reactions.

Results and discussion,

Glucose mutarotation and Raman spectral considerations

For the quantitative estimation of the anomeric species distribution of glucose in aqueous solutions, many methods have been reported in the open literature. Besides the well-established polarimetric method, molecular spectroscopic techniques have proven to provide comparable and accurate results[11]. Vibrational spectroscopies, Raman and FTIR, have

[a] Department of Chemical and Biochemical Engineering, Rutgers, The State University of New Jersey, Piscataway, 08854, NJ, USA

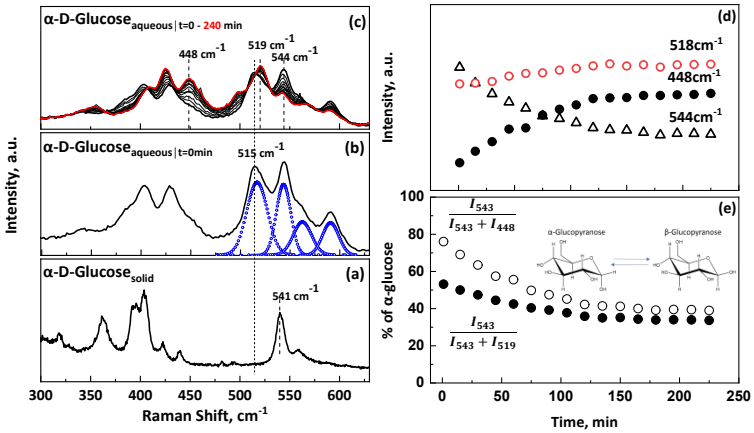

Figure 1: Raman spectrum of α-glucose in a) solid, b) water and c) under mutarotation reaction. Analysis of spectra is shown in d) and e).

been routinely used to study also solid-state glucose mutarotation reactions, solvent and cation effects on the anomeric equilibrium etc. In situ Raman detection of solid state glucose mutarotation has been also reported, but a spectral deconvolution using Gaussian peaks required thus making the analysis time consuming. For Raman spectroscopy, the well-accepted method proposed by Mathlouthi et.al. involves the ratio of the C_2-C_1-O_1 bending mode of the α- and β- anomer, i.e. $I_{543}/(I_{543}+I_{520})$, for the calculation of the anomeric equilibrium[12]. Although this ratio well estimates the anomeric equilibrium, spectral overlapping limits the accuracy of the method in the whole kinetic profile. This limitation can be overcome by rationalizing the vibrational assignments of the pure aqueous glucose anomers via study of their kinetic profiles, as discussed next.

In Figure 1a, we show for comparison the Raman spectrum of crystalline glucose used. The 541cm^{-1} band is characteristic to the contribution of C_2-C_1-O_1 bending mode of the α-anomer of glucose. The corresponding C_2-C_1-O_1 bending mode of the β-anomer is expected to give rise at 518cm^{-1}, which is absent in our crystalline sample, confirming the purity of the sample used. Upon dissolution in water, Figure 1b, characteristic bands of α-glucose (t=0min) become broader and shift slightly to higher frequencies. A noticeable change encompasses the appearance of a new band at 515cm^{-1} that almost coexist in frequency with the suggested C_2-C_1-O_1 bending mode of the β-anomer (518cm^{-1}). Since the spectrum was taken after complete glucose dissolution (t=0min indicates the time of collection of the first spectrum and not the time of mixing) one expects a small progress in glucose mutarotation to result in the formation of β-anomers that can overlap in the Raman spectra. However, we support that the 515cm^{-1} peak is characteristic of the α-anomer of glucose since the Raman kinetic data reported in Figure 1c shows a slight decrease of the intensity of the 515cm^{-1} and the appearance of a neighboring band at 519cm^{-1} with time. The previous argument is also supported by the clear isosbestic points which appear around the 515cm^{-1} band confirming a clear transition of α- to β- anomers with time.

The spectral envelop within the 200–600cm^{-1} range is sensitive to conformational changes of aqueous monosaccharides (and polysaccharides) since usually more than one vibrational motions contribute to each observed peak[13]. Theoretical calculation of the vibrational modes of glucose as well as experimental Raman/IR and Raman Optical Activity measurements have shown that skeletal endocyclic and exocyclic modes might coexist with bands that usually are dealt as "purely" anomeric modes. Corbett et.al.[14] studied the vibrational modes of "wet" α-D-glucose and suggested that the 538cm^{-1} band is conformational sensitive and upon interaction with water shifts to 512cm^{-1} and 522cm^{-1}. This is further supported by the work of Mathlouthi et.al where modes involving vibration of the CH_2 group show shifts in frequencies more than ~10 cm^{-1} upon changing D-glucose (or sucrose) concentration[15]. A deconvolution of the 500-600cm^{-1} range in our spectra show four peaks located at 515, 544, 564 and 590cm^{-1} which is in very good agreement with those reported in literature. Theoretical studies via first principle calculations can shed more light into how the interactions of glucose with water molecules can affect the vibrational modes observed.

In Figure 1c we show the in-situ Raman of the aqueous α-D-glucose solution as it undergoes mutarotation in the 300-650cm^{-1} range. Since all the spectra presented herein correspond to glucose in aqueous solutions, the spectral contribution from water as well as quartz cuvette used has been subtracted. In addition, prior to the subtraction, all the spectra have been normalized with respect to the total area of each spectrum. As the mutarotation reaction progresses, new Raman bands at 425, 448 and 519cm^{-1} evolve at the expense of those bands that correspond to the α-anomer of glucose. The band located at 448cm^{-1} (C-C-O skeletal mode as well[13, 15]), has almost no spectral overlap from neighbouring bands and thus we have used this peak as characteristic for the β-anomer instead of the 520cm^{-1}. As it can be seen in Figure 1d, the relative intensity of the 518 and 544cm^{-1} bands at early reaction time is almost identical indicating that the ratio $I_{543}/(I_{543}+I_{520})$ underpredicts the % change of the α-anomer at the beginning. This limits significantly our ability to accurately measure the anomeric concentrations that could potential help us to understand the catalytic behavior in downstream reactions, such as isomerization, dehydration etc. This is also shown in Figure 1e (solid circles). After 200min of reaction, this ratio predicts ~34% α- and ~66% β- anomers which in agreement with the expected equilibrium level[16]. Research on the solid state mutarotation of crystalline and amorphous glucose by means of

in-situ Raman spectroscopy has shown that the $I_{543}/(I_{543}+I_{520})$ ratio captures the kinetic profiles in the whole range[17]. This is achieved probably due to the fact that in solid state, α-glucose does not present the same conformational flexibility, possible hydrogen bonding or multiple configurations and thus no overlap in the characteristic 520cm^{-1} band of β-anomer appeared. Herein, we show that by utilizing the 448cm^{-1} as characteristic of the β-anomer of glucose that clearly appears with the same rate that the corresponding α-anomer disappears, we predict accurately both the early as well as late stages of the mutarotation reaction in liquid phase which is in excellent agreement with literature reported kinetic data in water. Thus, all the Raman spectra shown here have been analyzed with respect to the $I_{543}/(I_{543}+I_{448})$ ratio.

Effect of metal chlorides on glucose mutarotation

In Figure 2, we present the Raman spectra of aqueous glucose solutions under mutarotation reaction in the presence of 50mM of $AlCl_3$, $CrCl_3$ and $SnCl_4$. The in-situ Raman spectra under different catalyst concentration are not shown here for brevity (see supporting information). Upon addition of metal chlorides in glucose aqueous solution, we observe a clear change in the kinetics of mutarotation between $AlCl_3$, $CrCl_3$ and $SnCl_4$. Particularly, $SnCl_4$ facilitates glucose mutarotation much faster than the other metal salts under same concentration. The kinetics of glucose mutarotation become even faster at concentrations that reach 100mM for both catalysts, with $SnCl_4$ to exhibit always the highest rates based on the relative disappearance of relevant bands for α- and β- anomers. In the case of 100mM $CrCl_3$, the observed kinetics of mutarotation is fast as well (see rate constants at supporting information). By utilizing the $I_{543}/(I_{543}+I_{448})$ ratio as described earlier, in Figure 3(a-c), we present the kinetic profiles of glucose mutarotation as described by the change in α-anomer, in the range of 10mM-100mM catalyst concentration and compare with the rates in neat water. Conducting glucose mutarotation reaction in 10-50mM $AlCl_3$ we observe similar rates with neat water, while increasing the concentration to 100mM, we reach equilibrium approximately 50min faster. Our observation regarding the effect of $AlCl_3$ on mutarotation rates is in agreement with those reported by Hu and co-workers[18], where enhanced mutarotation rates (at room temperature) observed via ATR-FTIR spectroscopy. In this work, it was suggested that the presence of $[Al(OH)_{2(aq)}]^+$ species promotes both glucose ring opening/closing reactions (mutarotation) and glucose isomerization to fructose. The same group recently confirmed their previous argument regarding the existence of $[Al(OH)_{2(aq)}]^+$ species under these reaction conditions by using Electrospray Ionization−Mass Spectroscopy (ESI-MS) coupled with infrared spectroscopy[19]. Vlachos and co-workers have shown by coupling pH measurements, speciation model prediction with qNMR and dynamic light scattering techniques that the same partially hydrolyzed aluminum species is also the active species for glucose isomerization to fructose[20]. In contrast, the concentration of $SnCl_4$ appears to have a monotonic effect on glucose mutarotation rates, i.e. the higher the concentration of $SnCl_4$, the higher the rate of mutarotation. We believe that the

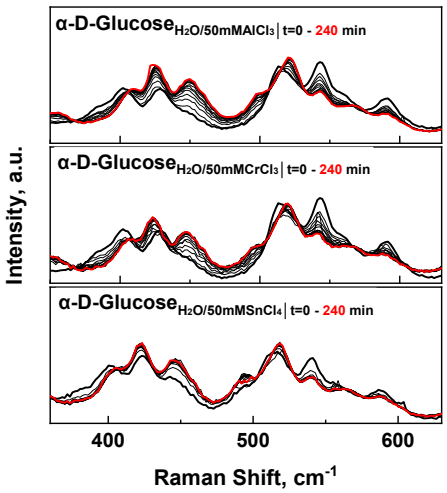

Figure 1: In situ Raman spectra of glucose mutarotation reaction

enhanced rates observed are due to competitive effect of Brønsted and Lewis acidity. Upon dissociation of metal chlorides in water into Me^{z+} and Cl^-, the $[M(OH_2)_n]^{z+}$ species will undergo hydrolysis and protons will be released as follows:

$$[M(OH_2)_n]^{z+} + xH_2O \leftrightarrow [M(OH)_x(OH_2)_{n-x}]^{(z-x)+} + xH_3O^+$$

Specifically, when $SnCl_4$ is dissolved in water, the hexa-aqua $[Sn(OH)_x(H_2O)_{6-x}]^{(4-x)+}$ complex dominates the solution at concentration below 100mM (concentration range of this study)[21]. Mesmer et.al. have shown that the hydrolysis of aluminum ion is kinetically slow at temperatures pertinent to our work, indicating that the pH of $AlCl_3$ solutions will be fairly stable throughout the reaction. The pH of the solutions at different stages of the experiments are listed in table S2. We clearly see that for the case of $SnCl_4$, the rate of glucose mutarotation correlates very well with pH values; the lower the pH, the faster the rate. This is in agreement with the proposed general acid catalyzed mechanism for this reaction. We also support this argument by conducting the mutarotation in the presence of Brønsted acids and analyzing their relevant kinetics (Figure s3). However, considering solutions with similar pH~2.9 (50mM $CrCl_3$ and 100mM $AlCl_3$), we observe that in $AlCl_3$, the observed rate values as reported in Table S1 are much higher than in $CrCl_3$ underscoring that the nature of salt used plays an important role on the mutarotation reaction at the low Brønsted acidity regime. Since the reaction mechanism might occur via a stepwise or concerted mechanism where two proton transfers are involved[22, 23], the nature of salt species in the local environment around glucose can potentially affect the transition state thus affecting the observed rates. However, further mechanistic work involving first principle calculations, molecular dynamics study as well as more advanced spectroscopic techniques is needed in order to disentangle the effect of the aqueous species in facilitating ring opening and closing of glucose as compared to Brønsted acids.

It is noteworthy here that, we did not observe any significant change in the equilibrium of α- and β- glucose anomers for $AlCl_3$ and $SnCl_4$. In all cases, ~35-40% α- anomer and 60-65% β-anomer were present at equilibrium. However, a monotonic increase in the percentage of the α-anomer was observed upon increasing the concentration of $CrCl_3$. Interestingly, at 100mM $CrCl_3$, the percentage of α-anomer increased to almost 50% as opposed to ~34% in neat water. In the pioneering work by Zhang and co-workers, it was inferred that $CrCl_3$ might stabilize the α-anomer thus accelerating isomerization rates[7]. However, since the present data pertain to room temperature, no direct conclusions can be drawn quickly with respect to temperatures pertinent to isomerization reaction. In order to bridge the temperature gap in the proposed approach, future research work pertaining to the rational design of high temperature optical liquid phase reactors in conjunction with mathematical handling of highly overlapping spectra (e.g. Principal Component Analysis and/or 2D correlation Raman spectroscopy) is considered an essential element. Although our Raman data provide useful qualitative as well as quantitative information regarding the changes occurring in the mutarotation reaction of glucose in the presence of metal chlorides, utilizing other spectroscopic techniques, such as NMR, can provide more insights into the actual anomeric distribution (pyranoses vs. furanoses and open chain) in equilibrium as well as interactions between glucose and active species at higher temperatures.

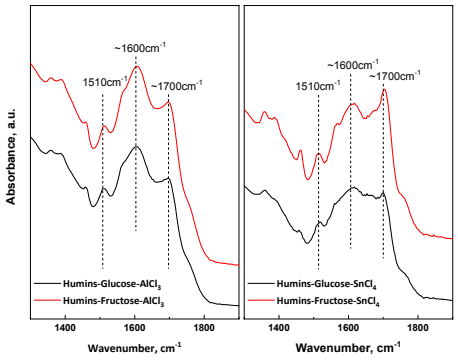

Figure 4: ATR-FTIR spectra of humins formed in $AlCl_3$ and $SnCl_4$ solutions

Effect of metal chlorides on humins molecular structure

There are many experimental and theoretical evidences in the open literature suggesting that the interaction of the aqueous metal species with sugars and/or furanic compounds can lead to enhance rates towards byproducts, such as humins. Understanding byproduct formation in biomass conversion is an essential component either in process optimization or in byproduct valorization. We have performed sugar degradation reactions (either with glucose or fructose) to intentionally produce humins for further study. The reaction time was 24-48hr to ensure high conversion of sugars at 120°C. The ATR-FTIR spectra of humins (Figure 4) revealed significant differences in the wavenumber range of 1300-1900cm^{-1}. We report that humins that formed in glucose and fructose in the presence of $AlCl_3$ appear to have similar molecular structure. However, in the presence of $SnCl_4$, we observe changes in the relative absorbance of the peaks located at ~1600 and ~1700cm^{-1} which are ascribed to C=C and C=O stretching modes[24-26]. This observation indicates that in humins prepared in $AlCl_3$, substituted furans are present as underscored by the 1600cm^{-1} band that could be arise via the HMF route. However, in $SnCl_4$ the 1700cm^{-1} band indicates the presence of C=O modes probably due to incorporation of carboxylic acids, aldehydes and ketones[24]. We hypothesize that the ease of ring opening of glucose in conjunction with the intrinsic acidity of $SnCl_4$ solutions lead possibly to the formation of those intermediates which in turn promote the formation of humins at early stages

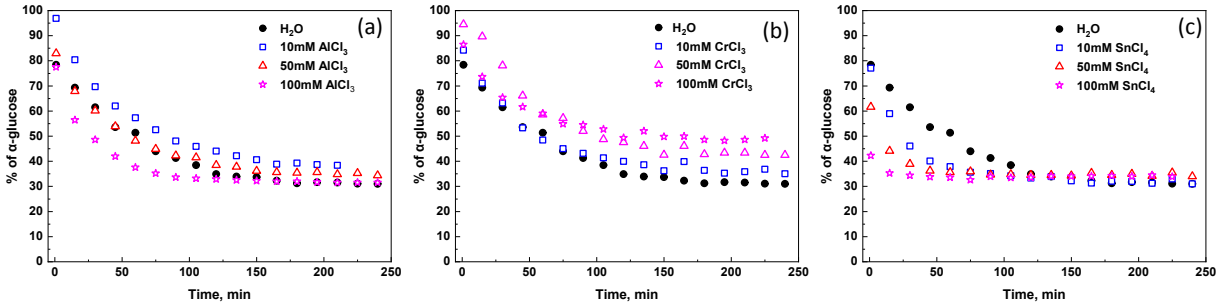

Figure 3: Kinetics profiles from in-situ Raman spectroscopic data. Analysis has been performed by utilizing the $I_{543}/(I_{543}+I_{448})$ ratio of skeletal modes of glucose

of reaction without passing the "HMF to DHH route". This argument is further supported by the small spectral contribution of furan rings (~1520cm^{-1}) in $SnCl_4$ as opposed to $AlCl_3$ derived glucose humins. When fructose is used as reactant, both $AlCl_3$ and $SnCl_4$ show the characteristic C=C stretching of furanic rings indicating that the HMF degrades to humins.

Conclusions

We have used in-situ Raman spectroscopy in liquid phase, to monitor glucose mutarotation reaction. We find that the rates follow the order of $AlCl_3$<$CrCl_3$<$SnCl_4$. Interestingly, we find that the presence of $CrCl_3$, promotes the formation of α-glucose anomer probably due to strong interaction of glucose and the dissolved metal species. We also show that the molecular structure of humins made in $AlCl_3$ and $SnCl_4$ are quite different; $AlCl_3$ species promote the pathway that involves incorporation of furan rings (possibly HMF to DHH) while $SnCl_4$ promote probably fragmentation of glucose and fructose prior to the formation of HMF.

Acknowledgements

This material is based upon work supported in part by Rutgers, The State University of New Jersey and the National Science Foundation Award #1705825.

Conflicts of interest

There are no conflicts to declare.

Notes and references

1. I. Delidovich and R. Palkovits, *Chemsuschem*, 2016, **9**, 547-561.
2. H. Li, S. Yang, S. Saravanamurugan and A. Riisager, *Acs Catalysis*, 2017, **7**, 3010-3029.
3. J. N. Chheda, G. W. Huber and J. A. Dumesic, *Angewandte Chemie International Edition*, 2007, **46**, 7164-7183.
4. Y. Román-Leshkov, C. J. Barrett, Z. Y. Liu and J. A. Dumesic, *Nature*, 2007, **447**, 982.
5. Y. Roman-Leshkov, M. Moliner, J. A. Labinger and M. E. Davis, *Angew Chem Int Ed Engl*, 2010, **49**, 8954-8957.
6. E. A. Pidko, V. Degirmenci and E. J. M. Hensen, *Chemcatchem*, 2012, **4**, 1263-1271.
7. H. B. Zhao, J. E. Holladay, H. Brown and Z. C. Zhang, *Science*, 2007, **316**, 1597-1600.
8. B. Wurster and B. Hess, *FEBS Letters*, 1974, **40**, S105-S111.
9. H. S. Lee and J. Hong, *J Biotechnol*, 2000, **84**, 145-153.
10. V. Choudhary, S. H. Mushrif, C. Ho, A. Anderko, V. Nikolakis, N. S. Marinkovic, A. I. Frenkel, S. I. Sandler and D. G. Vlachos, *J Am Chem Soc*, 2013, **135**, 3997-4006.
11. W. Pigman and H. S. Isbell, *Advances in carbohydrate chemistry.*, 1968, **23**, 11-57.
12. M. Mathlouthi and D. V. Luu, *Carbohydrate Research*, 1980, **81**, 203-212.
13. E. Wiercigroch, E. Szafraniec, K. Czamara, M. Z. Pacia, K. Majzner, K. Kochan, A. Kaczor, M. Baranska and K. Malek, *Spectrochimica Acta Part A: Molecular and Biomolecular Spectroscopy*, 2017, **185**, 317-335.
14. E. C. Corbett, V. Zichy, J. Goral and C. Passingham, *Spectrochimica Acta Part A: Molecular Spectroscopy*, 1991, **47**, 1399-1411.
15. M. Mathlouthi, C. Luu, A. M. Meffroybiget and D. V. Luu, *Carbohydrate Research*, 1980, **81**, 213-223.
16. N. Le Barc'H, J. M. Grossel, P. Looten and M. Mathlouthi, *Food Chem*, 2001, **74**, 119-124.
17. N. Dujardin, E. Dudognon, J. F. Willart, A. Hedoux, Y. Guinet, L. Paccou and M. Descamps, *J Phys Chem B*, 2011, **115**, 1698-1705.
18. J. Tang, X. Guo, L. Zhu and C. Hu, *ACS Catalysis*, 2015, **5**, 5097-5103.
19. J. Tang, L. Zhu, X. Fu, J. Dai, X. Guo and C. Hu, *ACS Catalysis*, 2016, **7**, 256-266.
20. Angela M. Norton, H. Nguyen, N. L. Xiao and D. G. Vlachos, *RSC Advances*, 2018, **8**, 17101-17109.
21. K. R. Enslow and A. T. Bell, *Catalysis Science & Technology*, 2015, **5**, 2839-2847.
22. P. Wlodarczyk, M. Paluch, A. Wlodarczyk and M. Hyra, *Phys Chem Chem Phys*, 2014, **16**, 4694-4698.
23. N. M. Ballash and E. B. Robertson, *Can J Chem*, 1973, **51**, 556-564.
24. I. van Zandvoort, Y. Wang, C. B. Rasrendra, E. R. H. van Eck, P. C. A. Bruijnincx, H. J. Heeres and B. M. Weckhuysen, *ChemSusChem*, 2013, **6**, 1745-1758.
25. Z. W. Cheng, J. L. Everhart, G. Tsilomelekis, V. Nikolakis, B. Saha and D. G. Vlachos, *Green Chem*, 2018, **20**, 997-1006.
26. G. Tsilomelekis, M. J. Orella, Z. X. Lin, Z. W. Cheng, W. Q. Zheng, V. Nikolakis and D. G. Vlachos, *Green Chem*, 2016, **18**, 1983-1993.